Polydimethylsiloxane and polyisoprene-based graphene composites for strain-sensing

Jorge A. Catalán
Department of Metallurgical, Materials and Biomedical Engineering, University of Texas at El Paso, El Paso, Texas 79968

Anupama B. Kaul[a)]
Department of Electrical and Computer Engineering, University of Texas at El Paso, El Paso, Texas 79968

(Received 15 January 2017; accepted 21 March 2017; published 31 March 2017)

In this paper, different composite materials have been developed and characterized for different applications in the health science field and as optoelectromechanical sensors. In this work, the authors have focused on two different types of composite materials. The first one having a matrix of polyisoprene (main component of natural rubber band) and the other with a matrix of polydimethylsiloxane, which is a biocompatible elastomer. Three different two-dimensional (2D) materials such as graphene, MoS_2, and WS_2 have been used as fillers in this study. In order to develop these composite materials, the authors used a solvent based exfoliation-processing technique in order to reduce the size of the tactoids of the 2D materials, to later on implement them into the different matrixes. *N*-methyl-2-pyrrolidone has been our selected solvent for the exfoliation process since it has been reported as one of the most effective solvents in the exfoliation process. Using some designed features, the authors were able to characterize the electrical properties of the composites as a function of strain or deformation, which the authors report on in more detail here.
 [http://dx.doi.org/10.1116/1.4979603]

I. INTRODUCTION

The world of two-dimensional materials, a current hot topic, is a place with current and upcoming frontiers. The recent discovery of graphene at the University of Manchester in 2004,[1] leads to the surprising conclusion that thin flakes/sheets of materials, in a range of a few atoms thick, can be stabilized. This experimental approach unveiled a new domain of outstanding and novel materials with surprising applications and properties that can guide the human society to take a huge step in the technology and science. In fact, some of these flourishing applications translate to solar cells, ultracapacitors, capacitive sensors, nanoelectronics, flexible electronics, transparent conductive electrodes, and some touch screens as well.[2–8] Although graphene has a wide range of novel properties,[9] it also has tough barriers that need to be overcome. One of the alternatives that came up to solve these issues was to look up for materials that share similarities with graphite and graphene. Certainly, a group of materials such as hexagonal boron nitride and transition metal dichalcogenides (TMDCs) stood higher than any others since they have very similar properties in the layer form.[10–12] TMDCs are compound materials formed by a transition metal (from IV B, V B, and VI B families of the periodic table) and a chalcogen such as S, Se, and Te. In fact, these materials were used as dried lubricants since the 1960s.[10] Some of these TMDCs show an intriguing bandgap transition, from indirect bandgap to direct bandgap, when being processed from their bulk form to their layered state.[8] The direct band gap makes these materials suitable for electronic device applications in the semiconductor industry.

Another important aspect that put TMDCs and layered materials in the scope of these recent years is the ease with which they can be processed. The key of their processing rests on their chemical bonding. The *intralayer* covalent bonding interaction and the weak *interlayer* interactions produced by van der Waal forces have led to simple ways to process these materials. These processing techniques have been divided into two main categories: top-down and bottom up approaches. An example of a top down approach is mechanical exfoliation, where a 2D material is peeled from the bulk crystal to their layer form with the help of conventional scotch tape. For the bottom up approach, chemical vapor deposition is one of the most common methods used nowadays. All these approaches have their advantages and disadvantages, since some of them can have low yields, poor quality, or they are expensive. One approach that is slowly getting more and more attention is the solvent-based exfoliation.[12,16,17] A top-down approach can be accomplished with the help of a solvent and a generated turbulent flow exfoliation of the bulk material. Coleman *et al.*[13–15] and others[16–18] have dedicated much of their efforts in providing information regarding different solvents such as cyclohexanone, *N*-methyl-pyrrolidinone (NMP), dimethylformamide, isopropanol (IPA), and dimethylacetamide for this solution-based technique.

The aim of this study is to provide some information that is useful in the understanding and explanation of some of the interactions of these TMDCs and layered materials with different polymers such as polyisoprene and poly-dimethylsiloxane. This is with the intention to expand the suitable applications of 2D materials as filler particles in polymer matrix composites. Ruoff and coworkers have focused their early work on composite materials, where graphene and materials similar to graphene are used as filler particles.[19–21]

[a)]Electronic mail: akaul@utep.edu

Graphene and other allotropes of carbon have been used in the fabrication of different transparent and stretchable devices such as field-effect transistor for wireless monitoring sensors,[22] devices integrated with a network of sensors that are capable of monitoring and sensing toxic gases.[23] In the same way, different materials such as silver nanowire composites have been utilized as wearable heaters for treating joint injuries,[24,25] expanding the possible applications of these flexible devices to the health science field. Solvent-based exfoliation was the selected technique to process our 2D materials from bulk to single and multilayers, where detail procedures used for the processing of these composites are presented. Also, different characterization techniques such as SEM, electrical characterization with the help of a micromanipulator, and a semiconductor parameter analyzer were implemented to provide information that was used to analyze and compare different composite materials that can be implemented as wearable electronics and health monitoring sensors.[26–32]

II. EXPERIMENTAL SECTION

A. Preparation of 2D materials dispersions

Raw material (as received powder) of graphite, MoS_2, WS_2, and aluminum was obtained from Sigma Aldrich. To make the dispersions, initial powder of each material was bath sonicated on an NMP solution, with the help of a Branson 4500H bath sonicator, at high power for different sonication times. These sonication times ranged from 0 h up to 18 h. The concentration of powder used for each of the materials mentioned above was 37.5 mg per ml of NMP. For maximal reliability, dispersions of graphite, MoS_2, WS_2, and aluminum were divided into five different sets of samples, each of one corresponding to a specific sonication time (0 h, 30 min, 6, 12, and 18 h). Then, different characterization techniques were used to analyze each sample.

B. Fabrication of polyisoprene matrix composite (natural rubber band)

For the elastomer based composites, two different concentrations were taken into account. Two different loadings of 37.5 mg ml^{-1} (low concentration) and 75 mg ml^{-1} (high concentration) were used. In order to prepare the composites, we follow the procedure proposed in Ref. 33. There, commercial rubber bands were soaked in toluene for two hours to open up the crosslinks of the elastomer. After 2 h, the rubber bands are then transferred to a vial containing NMP and the sonicated powder material. The rubber bands are left inside the vials containing the dispersion for about two days; this is to allow the sonicated powder diffusing into the elastomer matrix. Then, the rubber bands are placed inside an oven at a temperature of 60 °C in order to remove all the NMP and water contained inside the band. After drying off the composites, silver paste (Pelco® Conductive Silver Paint, Product No: 16062) was used as electrical contact onto the composites for electrical measurements with the help of a micromanipulator and a Hewlett Packard Precision Semiconductor Parameter Analyzer 4156A while mounted on a fixture designed in our lab (Fig. 1).

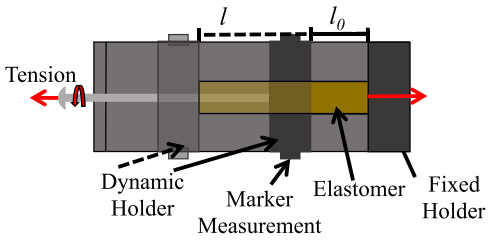

FIG. 1. (Color online) Schematic of the designed fixture used in the electrical characterization of the rubber band–graphene composite material. This device is designed so that the elastic band can be stretched and held at the stretched position, allowing electrical characterization with the micromanipulator. The dimensions of the fixture are as follows: length = 9.5 cm, width = 3 cm, and height = 2.5 cm.

C. Fabrication of PDMS matrix composite

Polydimethylsiloxane (PDMS) composite fabrication method is summarized as follows: The monomer (Sylgard 184 silicon elastomer Part No: NC9561957) is provided in the liquid form. The sonicated powder was mixed with the monomer, until uniform distribution was achieved. Then, curing agent was added and mixed with the monomer and sonicated powder mixture. This is to promote polymerization and formation of PDMS. Graphite and MoS_2 were the materials selected to reinforce the PDMS matrix; we discarded the WS_2 since it prevents the solidification/polymerization of the PDMS monomer once the curing agent/hardener is added. This decision was taken because during the first set of experiments with WS_2, a sudden release of energy in the form of heat (an exothermic reaction) took place once the curing agent was added. As mentioned before, this interaction prevented the solidification of the polymer, making us believe that 2D layer materials (depending on the amount added) can modify the polymer chain. Further analysis using techniques such as differential scanning calorimetry would be necessary to provide a better understanding of the exact mechanisms and reasons for this behavior. Two different concentrations were considered in this case, 15 wt. % filler material and 20 wt. % filler material; these concentrations were selected since we have found the percolation threshold of the composite was around these values. First, we poured the liquid PDMS in an aluminum boat for measuring its mass. By following the 1:10 weight ratio of curing agent:PDMS, we added 10% of the current mass of the PDMS contained in the aluminum boat in the form of curing agent. Then, the respective mass of graphite and MoS_2 is added to the curing agent:PDMS mixture, and then, it is thoroughly stirred until uniform distribution is achieved. Once the mixture is done, we poured some of it on top of regular glass slides, and with the help of a spin coater (Laurell Technologies Corporation, Model WS-650MZ-23NPPB), we treated the samples at 250 rpm for 80 s. After that, the glass slides containing the spin coated PDMS composite were baked in an oven for 1 h at 100 °C in order to promote the partial crystallization/solidification of the PDMS composites.

III. RESULTS AND DISCUSSION

A. Structural characterization

With the help of the MicroTrac S3500, the *as received* powders of graphite, MoS_2, WS_2, and aluminum were analyzed at different sonication times (t_{sonic}): 0, 0.5, 6, 12, and 18 h. In order to do so, each sample of each material was prepared as explained in Sec. II. Then, each sample was transferred to IPA solution in order to start the examination with the Micro Trac system. This system utilizes three different lasers (two blue and one red) in order to quantify the size of different particles. The blue lasers and the red laser have a wavelength in the range of 360–480 nm and 625–700 nm, respectively. Subsequently, the dispersion was drop casted in silicon wafer (oxide thickness ≈ 270 nm) to perform SEM and Raman spectroscopy.

With the help of MATLAB software, we were able to analyze and correlate the particle size distribution of the as received powders to some known statistical distribution curves. Figure 2(a) shows the particle size distribution of the MoS_2 powder. From the graph, we can see that the average particle size of the MoS_2 is around ≈5–6 μm and the maximum particle size is about ≈40 μm. This particle size distribution fits the statistical model given by a Nagakami type distribution. In Fig. 2(b), the particle size distribution of WS_2 can be observed. In this case, the average particle size of the *as received* powder is about ≈12–18 μm, but the highest particle size is in the range of 150 μm. The statistical model fitting the particle size distribution curve is a Burr type distribution. *As received* graphite powder particle size distribution can be seen in Fig. 2(c). This graph indicates that the average particle size is about ≈850 μm and the largest particle has a diameter of about ≈1600 μm. In this case, an extreme value distribution is the one that best fits the particle size distribution. Last, we have the *as received* aluminum powder sample. The aluminum average particle size is about ≈18–24 μm, and the largest diameter particle was found to be around 200 μm [see Fig. 2(d)]. This time, a Birnbaum–Saunders distribution best fits the distribution. This is found to be interesting, since the Birnbaum–Sanders distribution (also known as fatigue life distribution) was initially designed to analyze particle size reduction due to fatigue failure mechanisms. From all the as received powders, the aluminum sample was the only one fitting a statistical model related to processing undergone by the material to achieve the final product.

B. Rubber band (elastomer) composite versus PDMS (elastomer) composite

Figures 3(i)–3(iii) show SEM pictures of graphite at different sonication times to actively see the graphite tactoids

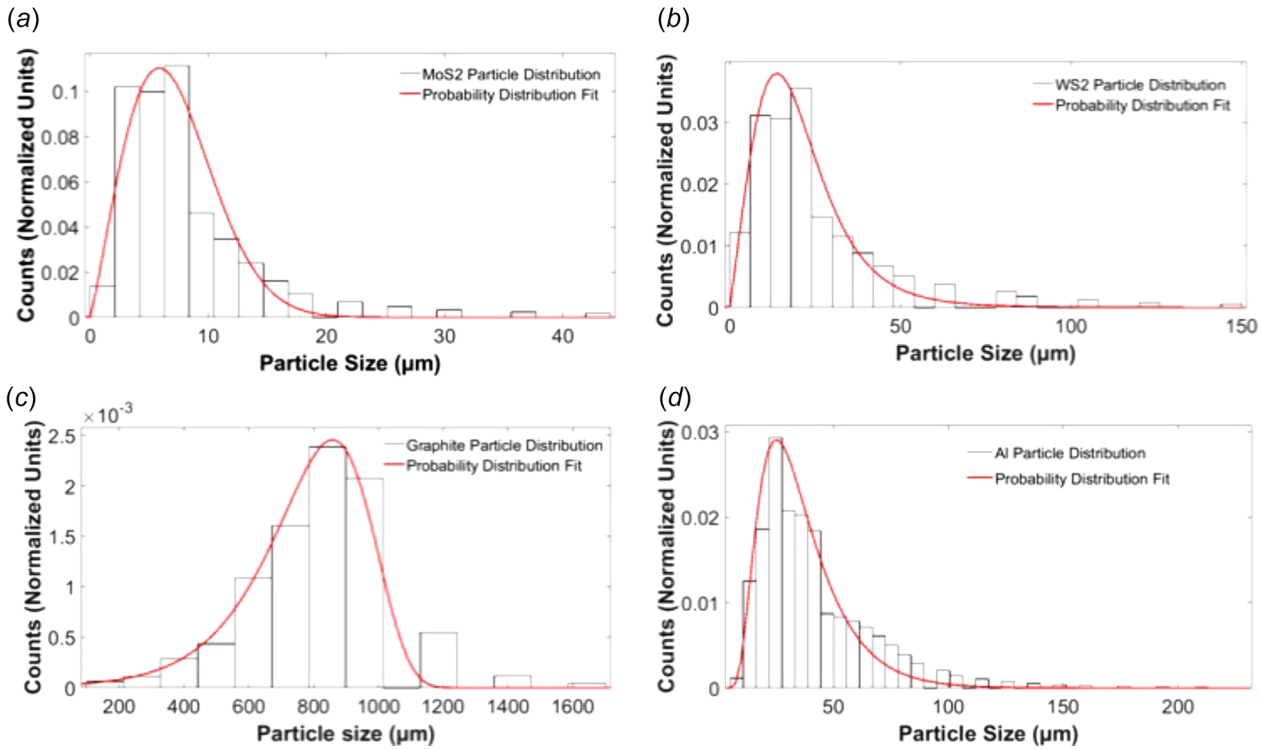

FIG. 2. (Color online) MATLAB software was used to analyze as received particle size data of the different materials used as fillers in the composites. With the software, we found the particle size distribution of the as received powders. While modeling, we found that different known statistical distributions were matching powder data. Some of these statistical distributions were not designed for particle size distribution, but they still match our data. (a) MoS_2 fits a Nagakami type distribution. (b) WS_2 fits a Burr distribution. (c) Graphite particle size distribution fits an extreme value distribution. From all four materials (graphite, MoS_2, WS_2, and aluminum), only aluminum showed a statistical distribution that in fact could talk about the processing method that the vendor/company used to provided the aluminum powder. (d) Aluminum showed a Birnbaum–Sanders distribution or fatigue life distribution. It is mostly related to failure times, but if we put it into context, this can provide us some information regarding the process they used to manufacture/decrease the particle size of the aluminum powder.

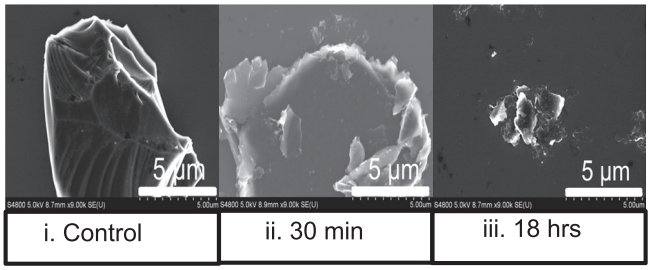

FIG. 3. SEM image of the graphite particles at different stages of sonication. (i) The *as received* graphite particle morphology. (ii) Flaking of the particles starts appearing. (iii) Noticeable particle size reduction from the initial condition. All pictures are at the same magnification (4800×).

breakdown into smaller tactoids or single layers. The 18 h sonicated graphite particles were used in the preparation of the composite materials. Refinement on the processing of the composites with materials other than graphite is needed in order to attain better results.

1. Electrical characterization

In this section, we used the fixture shown in Fig. 1 for measuring the current versus voltage behavior of the composite as a function of strain. In fact, rubber bands with graphene increase their resistance as the strain induced by the custom made fixture increases (Fig. 4).

2. Elastomer electrical properties comparison

Due to the fact that our polyisoprene (rubber band's main component) based composite material showed good response to the strain produced by the human body joints during motion, we decided to use a biocompatible polymer (PDMS) since any possible allergic reaction or skin irritation could be prevented by the use of it. In Fig. 5, there is a LogI vs V curve where both elastomer composites (rubber band and PDMS) are being compared. The blue lines (three lines at the top of the graph, and the noisy two lines at the bottom) represent the current passing through the PDMS-graphite composite at a specific strain induced by the motion of the finger as shown in Figs. 5(b)–5(f). The red lines (the five lines in between the top three lines and the two broken/noisy lines at the bottom of the chart) represent each of the current

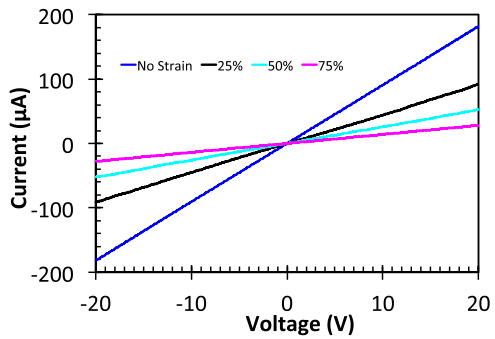

FIG. 4. (Color online) I–V curve of the polyisoprene–graphene composite material. This graph shows the electrical response to different strain levels ranging from 0% (no strain) up to 75% strain. Current intensity decreased as strain induced by fixture (Fig. 1) increased.

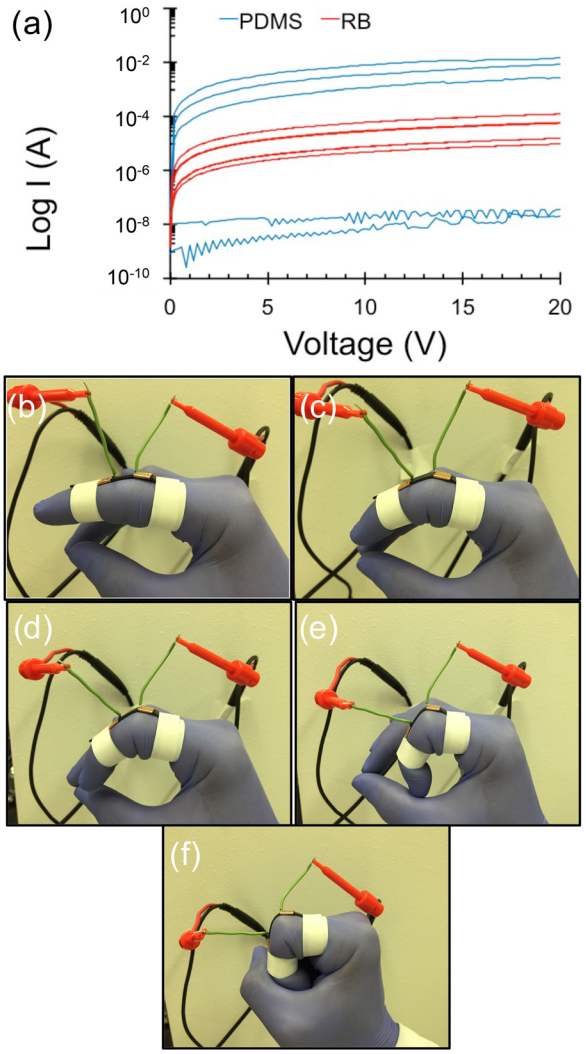

FIG. 5. (Color online) (a) I–V comparison between both elastomeric composites (PDMS matrix and polyisoprene matrix) in a log scale. Five measurements at different strain levels (b)–(f). The blue lines (three lines at the top of the graph, and the noisy two lines at the bottom) represent current response of PDMS material at different strain levels (b)–(f). (b) The strain induced into the sensor, which translates to the first line of both devices (blue and red). Equally, the red lines (the five lines in between the top three lines and the two broken/noisy lines at the bottom of the chart) represent current response of polyisoprene composite measurements (b)–(f). As the strain increased from (b) to (f), the current level passing through decreased. PDMS was only able to withstand three out of the five different strain levels. Irregular blue lines (the last two lines at the bottom of the graph) represent the failure of the composite at strain levels showed in (e) and (f), (f) representing the strain at the last line in (a) from top to bottom of both polymers.

levels of the rubber band-graphene composite at different strain levels. It can be said that the current is a few orders of magnitude higher for the PDMS-graphite composite, than for the rubber band composite. This can be attributed to the different fabrication process that each sensor undergoes. In the PDMS matrix composite, there are a much higher number of graphite particles allowing the charge carriers to go through. This is because the particles were directly mixed with the matrix material. On the other hand, the graphene–graphite particles that are touching each other is much less since these particles migrate inside the rubber band by

diffusion process once the crosslinks loose enough to have a high enough driving force for this to happen. The PDMS might allow a higher current to go through, but there is a strain level after which the current becomes much lower than the rubber band current at similar strain levels. This was expected since the strain produced by the third movement [Fig. 5(e)] ripped apart the matrix material since the elasticity of the PDMS is not as good as the elasticity of a rubber band. In fact, the elasticity of the PDMS heavily depends on the thickness of the sensor, the lower the thickness higher the elasticity. This can be attributed to the fact that at a much lower thickness, the molecules of this polymer can rearrange themselves in an easier way than when much more molecules are present (thicker sample).

IV. CONCLUSION

In this paper, chemically exfoliated particles of graphene can be used as filler material in polymer composites. With the help of toluene and a mixture of water and NMP, 2D particles can be diffused inside the matrix of a rubber band (mostly composed by polyisoprene). This composite material can be used as a strain sensor where we see the modulation of the current with mechanical deformation. We then also proceeded to form composites with a biocompatible elastomer material (PDMS). From this comparison, we conclude that the PDMS composite allows better current flow due to the fabrication procedure, but it does not exhibit nearly good elasticity as the rubber band composites.

ACKNOWLEDGMENTS

The authors would like to thank Alberto Delgado for his assistance with some of the measurements reported in this work. The authors also acknowledge the University of Texas System Faculty Science and Technology Acquisition and Retention (STARS) award (EC284802) for the acquisition of equipment in the establishment of the Nanomaterials and Devices Lab (NDL) at the University of Texas, El Paso (UTEP). The support from the Army Research Office (AROW911NF-15-1-0425) that enabled us to pursue this work is also acknowledged.

[1]K. S. Novoselov, A. K. Geim, S. V. Morozov, D. Jiang, Y. Zhang, S. V. Dubonos, I. V. Grigorieva, and A. A. Firsov, Science **306**, 666 (2004).
[2]P. Matyba, H. Yamaguchi, G. Eda, M. Chhowalla, L. Edman, and N. D. Robinson, ACS Nano **4**, 637 (2010).
[3]K. S. Novoselov, V. I. Fal'ko, L. Colombo, P. R. Gellert, M. G. Schwab, and K. Kim, Nature **490**, 192 (2012).
[4]E. W. Hill, A. K. Geim, K. Novoselov, F. Schedin, and P. Blake, IEEE Trans. Magn. **42**, 2694 (2006).
[5]H. B. Heersche, P. Jarillo-Herrero, J. B. Oostinga, L. M. K. Vandersypen, and A. F. Morpurgo, Nature **446**, 56 (2007).
[6]Q. H. Wang, K. Kalantar-Zadeh, A. Kis, J. N. Coleman, and M. S. Strano, Nat. Nanotechnol. **7**, 699 (2012).
[7]A. B. Kaul, J. Mater. Res. **29**, 348 (2014).
[8]D. Jariwala, V. K. Sangwan, L. J. Lauhon, T. J. Marks, and M. C. Hersam, ACS Nano **8**, 1102 (2014).
[9]A. K. Geim, Science **324**, 1530 (2009).
[10]A. D. Wilson and J. A. Yoffe, Adv. Phys. **18**, 193 (1969).
[11]A. K. Geim and K. S. Novoselov, Nat. Mater. **6**, 183 (2007).
[12]J. N. Coleman *et al*., Science **331**, 568 (2011).
[13]U. Khan, A. O'Neill, M. Lotya, S. De, and J. N. Coleman, Small **6**, 864 (2010).
[14]G. Cunningham, M. Lotya, C. S. Cucinotta, S. Sanvito, S. D. Bergin, R. Menzel, M. S. P. Shaffer, and J. N. Coleman, ACS Nano **6**, 3468 (2012).
[15]K. R. Paton *et al*., Nat. Mater. **13**, 624 (2014).
[16]A. Jawaid, D. Nepal, K. Park, M. Jespersen, A. Qualley, P. Mirau, L. F. Drummy, and R. A. Vaia, Chem. Mater. **28**, 337 (2016).
[17]B. J. Carey, T. Daeneke, E. P. Nguyen, and Y. Wang, Chem. Commun. **51**, 3770 (2015).
[18]S. Stankovich, R. D. Piner, X. Chen, N. Wu, S. T. Nguyen, and R. S. Ruoff, J. Mater. Chem. **16**, 155 (2006).
[19]S. Stankovich, D. A. Dikin, G. H. B. Dommett, K. M. Kohlhaas, E. J. Zimney, E. A. Stach, R. D. Piner, S. T. Nguyen, and R. S. Ruoff, Nature **442**, 282 (2006).
[20]P. Lu, X. Wu, W. Guo, and X. C. Zeng, Phys. Chem. Chem. Phys. **14**, 13035 (2012).
[21]E. Scalise, M. Houssa, G. Pourtois, V. Afanas'ev, and A. Stesmans, Nano Res. **5**, 43 (2012).
[22]J. Kim, M.-S. Lee, S. Jeon, M. Kim, S. Kim, K. Kim, F. Bien, S. Y. Hong, and J.-U. Park, Adv. Mater. **27**, 3292 (2015).
[23]K. Lee *et al*., Nano Lett. **14**, 2647 (2014).
[24]S. Choi *et al*., ACS Nano **9**, 6626 (2015).
[25]B. W. An, E.-J. Gwak, K. Kim, Y.-C. Kim, J. Jang, J.-Y. Kim, and J.-U. Park, Nano Lett. **16**, 471 (2016).
[26]S. Yao and Y. Zhu, Nanoscale **6**, 2345 (2014).
[27]A. Pantelopoulos and N. G. Bourbakis, IEEE Trans. Syst., Man Cybernetics, Part C **40**, 1 (2010).
[28]M. Kaltenbrunner *et al*., Nature **499**, 458 (2013).
[29]T. Yamada, Y. Hayamizu, Y. Yamamoto, Y. Yomogida, A. Izadi-Najafabadi, D. N. Futaba, and K. Hata, Nat. Nanotechnol. **6**, 296 (2011).
[30]M. Amjadi, A. Pichitpajongkit, S. Lee, S. Ryu, and I. Park, ACS Nano **8**, 5154 (2014).
[31]M. Hempel, D. Nezich, J. Kong, and M. Hofmann, Nano Lett. **12**, 5714 (2012).
[32]J. Botsis, L. Humbert, F. Colpo, and P. Giaccari, Opt. Lasers Eng. **43**, 491 (2005).
[33]C. S. Boland *et al*., ACS Nano **8**, 8819 (2014).